Systematic Modeling of Perturbations Effects in the Arterial Input Function with implication for DCE-MRI evaluation.

D. H. Wu[1,2], and R. Alam[2]

[1]Radiological Sciences, University of Oklahoma Health Science Center, Oklahoma City, Oklahoma, United States, [2]Computer Sciences, University of Oklahoma, Norman, Oklahoma, United States

Introduction: The application of Dynamic Contrast Enhancement of Magnetic Resonance Images (DCE-MRI) has a potentially vital role in pharmacological drug studies and functional tumor evaluation. Recently, there has been considerable interest in how the arterial input function (AIF) is applied in DCE-MRI. The various forms of analysis have led to controversy in its implementation. Recent reports of its use have demonstrated differences in within-subject coefficient of variations due to different types of AIF fitting functions [1]. Additionally, improved population-based strategies for the use of the AIF were also introduced [2]. It is known that DCE-MRI results may differ due to pulse sequence timings, injection rates, vascular supply within organs. This indicates that there is a current need for improved understanding and collaboration among centers concerning acquisition implementation. In an attempt to improve the understanding of the AIF, our focus concerned modeling, by both individual and group analysis, the perturbations in timing and use these to predict the effect on DCE-MRI tumor results. We specifically evaluated sensitivity to variations in:

1) timing shifts (delay and advance) interacting with perturbation changes due to dispersion effects (Individualized AIF)
2) bioexponential parameters of the AIF fit functions prior to DCE-MRI calculation (modeled AIF fit).
3) the average population estimate AIF, as applied to individualized estimates for both of the above techniques.

Method: 42 cervical cancer patients with individualized measurements of AIF were evaluated. Tumor delineation was performed on a Matlab/Java based tumor delineation program that was developed in our laboratory. Manual delineation was performed on T2-Turbo spin echo (TSE) images and stored. DCE-MRI evaluation was performed on a 3D Spoiled FLASH-based sequence within these ROI across 10 time frames at 14s intervals. We applied a Tofts model to calculate k_{12}, k_{21} and amplitude using Marquart Levenberg nonlinear estimation of these pharmacokinetic parameters. To model the perturbations in the AIF, when time series is advanced or decreased more than one time point, we extrapolated for the values outside the window. Then, we interpolated in intervals of 0.25 of a time point to evaluate subtemporal shifts. Next, we applied time shifting to the resultant data while applying a convolution by a Gaussian with specified changes in full width half maximum (FWHM) to model dispersion. For our second goal, we applied a fit to each one of the AIF functions prior to calculation of the DCE-MRI pharmacokinetic parameters. We modified the formula by Yankeelov [3] to incorporate T0 as a shift vector and vary B for the dispersion effect.

$$C_p(t) = \alpha \cdot (t - T0) \cdot \exp(-(t - T0)/\beta) + \gamma[1 - \exp(-(t - T0)/\delta)] \cdot \exp(-t/\varepsilon) \qquad (1)$$

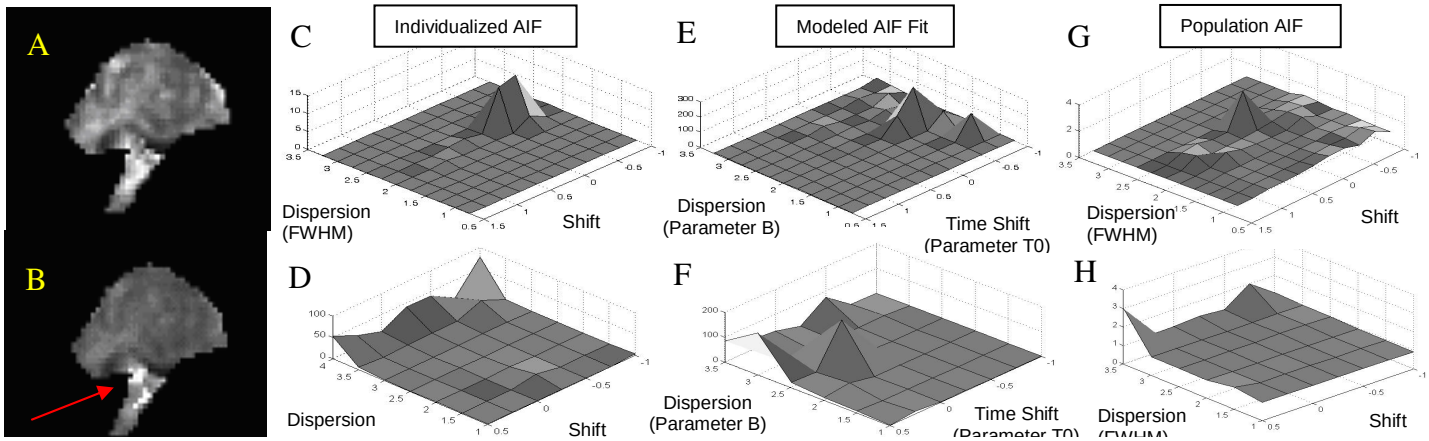

Fig. 1: A) A single slice of the DCE-MRI tumor data prior to any shift or dispersion is compared with B) time shift modulation of 0.75 of a sampling time interval and a FWHM of 2 time pts Gaussian. C) Variations from time shift and dispersions within a single individualized AIF patient case and D) Average Variation Map across 42 patients each with their individualized AIF. (E) Results from Individualized patient fit function (see equation (1) over one patient and F) corresponding average variation over 42 patients with the fitted AIF relationship using equation 1. G) DCE-MRI results from an individual and H) 42 patient population averaged effect that uses a single population based AIF (which is averaged over all patients) for the analysis. All results above reflect ratio changes in K_{12} (as averaged across the entire slices of the tumor). In summary top row C,E,G are from a single individual and bottom row D,F,H are the DCE-MRI results averaged over 42 patients.

Results: Fig. 1 A and B illustrate the images from the original after phase shifts and dispersion in the AIF. Of note, there is some instability in 'hot' regions as illustrated by the red arrow in fig 1. We also have examined results across the 3 test conditions (individualized AIF, modeled fit of AIF prior to analysis, and averaged population AIF). Figure 1 (C,E,G) represents the results of one individual subject, and are instructive as they illustrate the dependence on shift and dispersion parameters. In the same figure (D,F,H-bottom row) the plots are constructed similarly to C,E,G, with the exception that the results are averaged across 42 patients.

Discussion: Fig. 1 E & F illustrate the impact of regression of the model prior to DCE-MRI analysis, and illustrate the significant sensitivity to variation in the parametric coefficients of Eq. 1 (greater than 10 times the errors). Such results warrant careful attention when the Modeled AIF fit is used. It also appears that the population average (G&H) method appears to spread the errors across a greater range of parameter shifts (dispersion and temporal shifts) when compared to the individualized AIF (C and D). This can be interpreted as providing greater protection from variations in the application of the AIF. The systematic approach to modeling perturbations has led us to improved insight regarding our data and greater confidence in population-based AIF methods.

References:
1. Taylor ISMRM 2006: 2819,
2. Parker MRM 2006: 993-1000,
3. Yankeelov MRI 2005: 519-529